Real-Time PCR: A Review of Approaches to Data Analysis

D. V. Rebrikov and D. Yu. Trofimov

DNA-Technology JSC, Moscow, 115478 Russia
e-mail: denis@dna-technology.ru

Received December 28, 2005

Abstract—The registration of the accumulation of polymerase chain reaction (PCR) products in the course of amplification (real-time PCR) requires specific equipment, i.e., detecting amplifiers capable of recording the level of fluorescence in the reaction tube during amplicon formation. When the time of the reaction is complete, researchers are able to obtain DNA accumulation graphs. This review discusses the most promising algorithms of the analysis of real-time PCR curves and possible errors, caused by the software used or by operators' mistakes. The data included will assist researchers in understanding the features of a method to obtain more reliable results.

The polymerase chain reaction (PCR) with registration of DNA accumulation in the course of the reaction (in real time) has gained increasing acceptance as a laboratory technique suitable for both scientific and diagnostic purposes. The registration of DNA accumulation during the reaction makes it possible to avoid separating the readout stage, as well as rules out the possibility of laboratory contamination; in addition, the results obtained allow nucleic acids to be analyzed quantitatively as well as qualitatively [1]. Such tasks as assessment of the level of transcript representation and pathogen concentration and detection of single-nucleotide polymorphisms (SNPs) are accomplished much easier if a real-time PCR is used [2–7].

Real-time registration of the accumulation of PCR products requires specific equipment, i.e., detecting amplifiers capable of recording the level of fluorescence in the reaction tube. By the time the reaction is completed, a researcher using such an instrument obtains DNA accumulation graphs, in which the level of fluorescence is plotted against time (i.e., the number of amplification cycles; Fig. 1a).

Means for visualization of DNA accumulation during a PCR include the use of intercalating dyes, labeled primers or oligonucleotide probes, and combinations thereof [8–12].

An analysis of the results of a real-time PCR also involves several principally distinct methods [13–16]. Regardless of the exact method of analysis, a quantitative real-time PCR requires that graphs of DNA accumulation obtained from several samples be compared (e.g., a test sample may be compared to a standard sample or other test samples). The precision of the study on the whole will depend on whether such a comparison was performed correctly. The methods of curve comparison, currently offered by manufacturers of detecting amplifiers and software, differ considerably in both

precision and stability, particularly if the signal is weak. Here, not the absolute strength of the signal is in question (as a rule, the signals are high enough to be easily recorded by modern equipment), but its ratio to background fluorescence [17, 18].

A correct comparison requires that the graphs obtained using detecting amplifiers be normalized in a certain way, in order to decrease the effects of nonbiological factors (errors that occur while preparing reaction mixtures, a scatter of optical properties of the tubes, the heterogeneity of the optical system of detecting amplifiers, etc.).

Scientists and representatives of equipment manufacturers attend conferences on quantitative PCRs (qPCR), where they attempt to elaborate a common procedure standardizing both the layout of the experiment and the analysis of the results, with the goal of increasing the significance of the data. Such discussions are the subject of considerable attention at International qPCR Symposia and Application Workshops held annually. A unified procedure is expected to ensure that the results of the qPCR, generated in distinct laboratories using diverse amplifiers, be compared in a correct way [19]. It is unfortunate that such a procedure has not been adopted thus far; an optimum method of data analysis has not been selected. Several schemes for arranging real-time PCR experiments and methods for analyzing the data generated are currently being developed, from which approaches ensuring the best results should be derived in the near future [16, 20, 21].

A researcher today most frequently delegates the qPCR data analysis to software supplied with the equipment. However, the underlying algorithms by no means yield adequate results in all cases, because approaches to a reliable analysis of fluorescence accumulation curves are under development, and manufac-
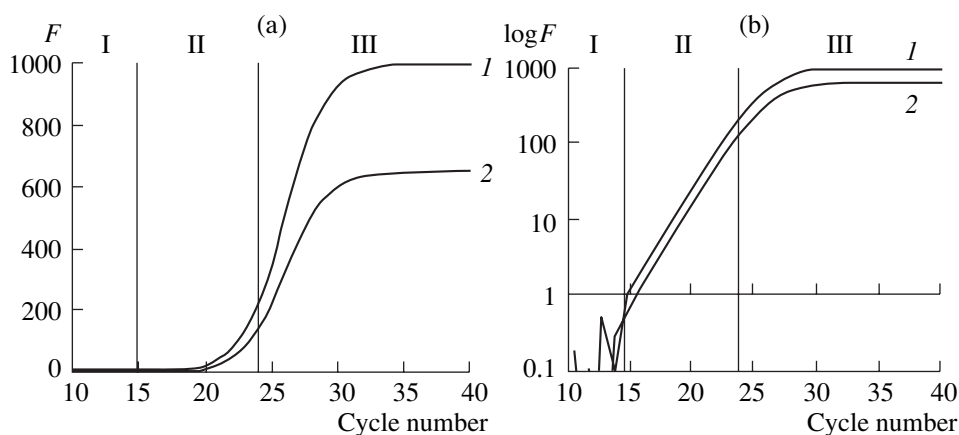
Fig. 1. Curves of DNA accumulation during a PCR, obtained for identical samples (PCR duplicates), presented as linear (a) and semilogarithmic (b) plots. The values of factor α for curves *1* and *2* are different. I, II, and III designate, respectively, the regions (segments) of noise, exponential increase, and plateau. *F* is the level of fluorescence.

turers of the equipment use diverse methods of analysis.

Nevertheless, the majority of software products make it possible to export raw data in a spreadsheet format (compatible with standard programs, such as Microsoft Excel), which opens up the possibility to analyze them using in-house approaches (not provided for by algorithms of the original software). In addition, there are several software packages, developed for such an alternative analysis of the real-time PCR results (e.g., DART-PCR, Q-Gene, and SoFAR) [22–24]. Clearly, it is possible to recommend to researchers the use manual approaches, in order to obtain more precise and reliable results now, without waiting for the incorporation of these algorithms into software packages supplied with detecting amplifiers.

In this work we analyze contemporary approaches to the mathematical processing of raw data obtained by real-time PCR, with an emphasis on the major problems encountered in analyzing DNA accumulation curves. As the correct use of new analytical algorithms requires a clear understanding of the possible effects of the PCR parameters, some of them are also reviewed.

PCR efficiency. The simplest PCR formula may be represented as follows: the amount of reaction products after cycle n is equal to the initial number of molecules multiplied by 2^n [25], i.e.,

$$N_n = N_0 2^n, \tag{1}$$

where n is the number of the reaction cycle; N_0 is the amount of primers at the onset of the reaction; N_n is the amount of the reaction products after the completion of cycle n; and two is the efficiency factor of the reaction (or just PCR efficiency).

This formula is valid upon the assumption that, following each cycle, the amount of the amplified molecules is doubled. Indeed under optimum conditions, the value of PCR efficiency nears two, even though in certain cases it may be considerably lower. Moreover, the efficiency factor fluctuates throughout the entire PCR, from the very first cycles to the end of the process where it rapidly falls to unity (because of the competition between the processes of primer annealing and reassociation of DNA fragments [26]).

Nevertheless, considering the efficiency to be largely constant throughout the process, the amount of DNA after cycle n may be expressed as follows:

$$N_n = N_0 E^n, \tag{2}$$

where E designates the efficiency of PCR.

The PCR efficiency is a number showing the increase (in times) in the amount of the amplified DNA fragments taking place during one cycle [27]. This parameter becomes extremely important when the PCR is used for quantitative determination of nucleic acids.

Contemporary publications provide two distinct definitions of PCR efficiency:

$N_n = N_0 E^n$, where $1 < E < 2$ (variant 1) [16, 22] and

$$N_n = N_0 (1 + E)^n, \tag{3}$$

where $0 < E < 1$ (variant 2) [24, 28].

The second variant was introduced by researchers to enable the efficiency to be expressed as a percentage; thus, in reading the literature on qPCRs, one should pay specific attention to the terminology used by the authors (the use in the literature of the second definition has recently become more frequent). In this work we will use the first variant of the definition, for the sake of simplifying the formulae.

The efficiency of the reaction exerts pronounced effects on the result of the amplification. Even slight changes in the efficiency lead to considerable differences in the data obtained [29, 30]. Thus, a 0.15 difference in the value of E translates, by the end of the 30th cycle, into a tenfold higher or lower yield of the product [31]. In practice the efficiency of the reaction remains

largely unchanged throughout the entire process, excluding the last cycles where the resources are rapidly exhausted and PCR cessation occurs. However, even minimum changes in the efficiency that occur while the reaction is taking place become notable when the samples used differ considerably in the initial template concentration. Moreover, the change in the efficiency is a variable, in that the longer the reaction lasts, the more pronounced is the drop in its efficiency (due to a decreases in the general activity of the enzyme and the concentrations of the reagents).

Parameters of the reaction. As a detecting amplifier measures a fluorescence signal (i.e., the function of the concentration of DNA in the tube) rather than DNA itself, a measurement of the latter requires knowledge of the relation of the concentration to the fluorescence intensity. It is conceivable that the fluorescence signal is proportional to the amount of DNA molecules in the reaction tube:

$$F = \alpha N, \tag{4}$$

where F is the fluorescence signal; α is an unknown factor; and N is the amount of DNA molecules.

Thus, by substituting (4) into (2), we obtain

$$F = \alpha N_0 E^n, \text{ [22]}. \tag{5}$$

The α factor may vary considerably from experiment to experiment (and even from tube to tube within the same experiment) [24, 32]. The factor depends on instrument settings, amplification tubes (type, transparency, and cleanness), the reagents used, etc. It is considerably affected by the choice of the system visualizing DNA accumulation (intercalating dyes, oligonucleotide probes, labeled primers, etc.).

Thus, a comparison of the data derived from distinct experiments (or tubes within the same experiment) cannot be performed directly, because the corresponding values of factor α may differ considerably. Curves recorded during the same experiment in two absolutely identical tubes may appear as those shown in Fig. 1a (several identical reactions are usually run in parallel, thus averaging the effects of random factors; such reactions are hereafter termed PCR duplicates).

The case where differences in the initial amount of DNA are mistaken for those in the values of factor α is worthy of separate treatment. Such mistakes may occur if a researcher preparing to run PCR duplicates introduces single copies of original DNA molecules into the tubes. As a result of fortuitous variations, the numbers of molecules added into absolutely identical tubes may differ severalfold, which is not taken into account in the subsequent data analysis [33–35].

A comparison of real-time PCR curves is based on the number of the cycle, at which a signal reliably recorded by the amplifier is generated, but not on the endpoint fluorescence intensity (as in the case of detection by electrophoresis in agarose gels). This threshold cycle (C_t) is also termed a crossing point (C_p) [4].

The use of a standard method for determining the threshold cycle (using the threshold line) shows that, in the case illustrated by Fig. 1a, the difference between C_t values of two identical samples will be significant (let alone the results of the endpoint detection). As follows from expression (5), the discrepancy in C_t values for two reactions may be caused by differences in (1) the initial concentration of DNA templates (N_0), (2) the reaction efficiency (E), or (3) the value of the α factor. A mathematical analysis of the curves makes it possible to separate cases caused by (2) and (3). If the graphs of Fig. 1a are depicted in semilogarithmic plots (i.e., if $\log F$ is the ordinate), the curves shown in Fig. 1b are obtained.

The formula describing these curves will be as follows:

$$\log F = \log \alpha + \log N_0 + n \log E, \text{ [36, 37]}. \tag{6}$$

As noted from Fig. 1b, in this case the curves may be superposed by moving them along the ordinate. This means that the efficiencies of the two reactions are equal, and the observed differences arise from the multiplication by dissimilar values of factor α (provided that the amount of DNA added into the tubes is identical) [38].

Let us now consider the DNA accumulation curves in greater detail. Each graph may be separated into three regions corresponding, respectively, to noises, the exponential phase, and the plateau (Fig. 1). The noises region is particularly well discernable in semilogarithmic plots (Fig. 1b), where the transformation used renders random fluctuations of low-fluorescence values considerably more visible. Within this interval the fluorescence signal is weaker than the noise of the measuring instrument, and it is not possible to record the signal reliably [36, 37]. The exponential region is characterized by confident registration of the signal (which exceeds the background considerably), and the product is accumulated with a constant efficiency (the E value remains largely unchanged), because of the excess of the reaction resources. When viewed in semilogarithmic plots (Fig. 1b), this region appears as a straight line. The reverse is also true: as long as the graph of DNA accumulation appears as a straight line in a semilogarithmic plot, the reaction efficiency remains unchanged, whereas the inflection point corresponds to its decrease. The exponential region is the best for comparing graphs (i.e., determining the threshold cycle, the reaction efficiency, etc.). In this case the results obtained are the most precise [36, 37]. The plateau is characterized by a drop in the reaction efficiency (largely due to competition of two processes, i.e., primer annealing and reassociation of the product formed) and eventual cessation of the process.

Determination of PCR efficiency. As efficiency is one of the most important PCR parameters, its correct determination makes it possible to increase the precision of qPCR tests. Although the majority of factory-
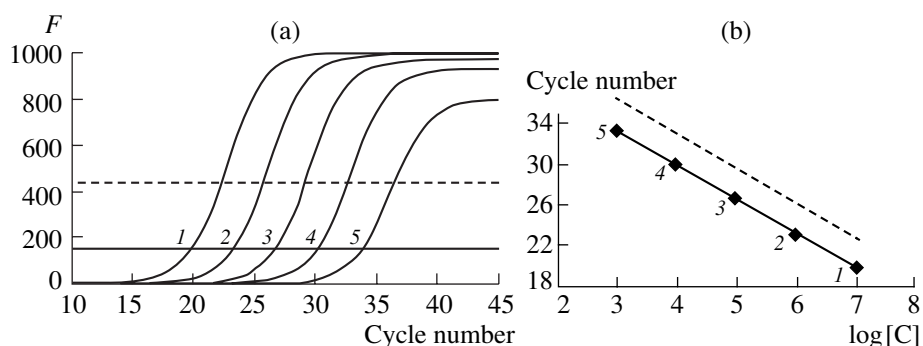
Fig. 2 Assessment of PCR efficiency using serial dilutions of the sample. a: Typical graphs (*1–5*) of DNA accumulation for serial dilutions of the sample under study (solid and dashed lines are variants of the threshold line. b: Dependence of the threshold cycle on the initial concentration of DNA, plotted based on the data of the curves depicted to the left.

preinstalled software packages detecting amplifiers do not make corrections for the efficiency of the reaction, the instrument designers seek to incorporate an estimation of E into standard algorithms of data analysis. Three different methods for determining PCR efficiency are described below.

Method 1: Serial dilutions. The efficiency of the reaction may be determined by running PCR on serial dilutions of the sample under study [16, 24, 28, 39, 40]. When the reactions are completed, the C_t values are determined for each dilution (e.g., using the threshold method; Fig. 2a). Thereafter, these values are used for obtaining $\log[C]/C_t$ plots (Fig. 2b), which are almost linear. Strictly speaking, the values will not necessarily lie along a straight line of the plot, because the values of the PCR efficiency for different dilutions may differ.

Let us describe the straight line shown in Fig. 2b by a general equation for straight lines:

$$y = -ax + b. \tag{7}$$

It is not difficult to see that the negative factor a demonstrates how many cycles it takes to increase one order of magnitude the fluorescence signal (i.e., amount of DNA). Therefore, the $1/a$ value shows the increment (in orders of magnitude) in DNA amount, achieved during one reaction cycle. To determine this increment, ten should be raised to the power $1/a$. As PCR efficiency is a number showing the increase (in times) in the amount of the amplified DNA fragments that takes place during one cycle, it is exactly the efficiency that is described by the expression below:

$$E = 10^{1/a}. \tag{8}$$

Thus, running PCR on serial dilutions of a sample and obtaining a standard straight line as described above makes it possible to determine the efficiency of the reaction by the slope of this line.

Method 2: Absolute fluorescence increment. The efficiency of the process may be determined without dilutions (methods 2 and 3). In method 2 E is determined using the exponential segment of the curve and simple techniques of data approximation. In method 3

(mathematical model fitting) the whole fluorescence accumulation plot is described using an equation.

So far several distinct approaches to calculating the reaction efficiency from the exponential segment of the curve have been reported [14, 15, 36, 37, 41, 42]. Here we provide only one such technique as an example [37]. In order to determine E, let us describe the straight segment of the semilogarithmic plot of a DNA accumulation curve (Fig. 1b) using a standard straight line equation:

$$y = cx + d.$$

Comparing equation (6) and the straight line equation makes it easy to note that factor c is identical to $\log E$. From this,

$$E = 10^c. \tag{9}$$

In practice, the following finding is useful: if the straight segments of the graphs shown in Fig. 1b are parallel, the E values for these reactions are identical.

Method 3: Mathematical model fitting. In recent years publications have appeared in the literature, which attempt to describe the shape of the whole graph of fluorescence accumulation by an equation [32, 43–46]. Consider the sigmoid model with four parameters proposed in [43] as an example. In this model the curve is described by the following equation:

$$f = y_0 + \frac{a}{1 + e^{-\left(\frac{x - x_0}{b}\right)}}, \tag{10}$$

where y_0 is the fluorescence baseline; a is the difference between the fluorescence maximum and the baseline; e is the base of Naperian logarithm and x is the number of the current cycle of the reaction; x_0 is the value of the first derivative maximum; and b is the slope of the curve.

The parameters taken into account in equation (10) are shown in Fig. 3. Although this approach does not allow the value of the reaction efficiency to be calculated, it makes a comparison of the E values, obtained
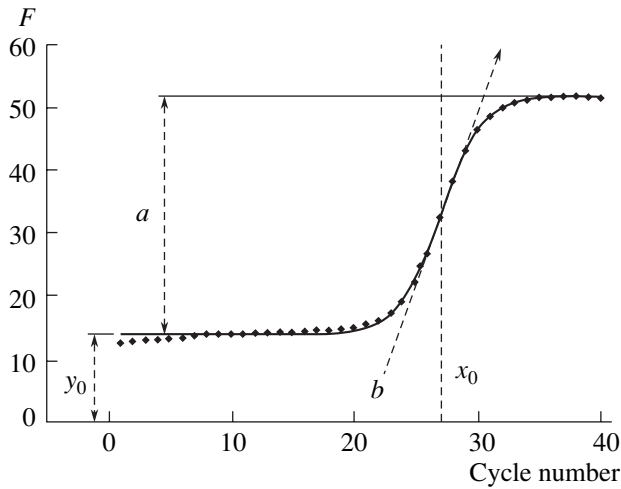
Fig. 3. Parameters of fluorescence accumulation curves, used in the sigmoid model with four parameters: y_0 is the fluorescence baseline; a is the difference between the fluorescence maximum and the baseline; x_0 is the value of the first derivative maximum; and b is the slope of the curve.

for two reactions, possible. The lower the value is of parameter b, the higher the efficiency is.

Thus, there are many ways to estimate PCR efficiency, which we separated into three groups, i.e., methods of (1) serial dilutions, (2) individual graph analysis (based on the rate of fluorescence accumulation within the exponential region), and (3) mathematical model fitting. Each approach has its advantages and drawbacks, and it is problematic to separate the algorithm and ensure the greatest precision. In practice, however, it is necessary to be able to estimate the reaction efficiency from a single curve. For this reason we expect that the subsequent development of data-analysis algorithms will be based on methods (2) and (3).

Processing of raw data. *Background subtraction.* Figure 4 shows typical raw graphs of DNA accumulation (fluorescence increase) during a PCR. As already indicated the intensity of fluorescence recorded by a detecting amplifier during the reaction may be described by formula (5). However, this formula does not take background fluorescence into account, which is always present in practice. The background inherent in real-time PCR experiments may be divided into components, of which one is a constant (b) and the other is a variable (kn) (equation 11). Strictly speaking, the variable component undergoes a nonlinear change during the reaction; nevertheless, to a first approximation, this change may be represented as a linear function:

$$F = \alpha N_0 E^n + b + kn, \qquad (11)$$

where b and kn are the constant and variable components of the background, respectively (the latter being a function of the cycle number).

A constant background is due to residual fluorescence of the dye, differences in tube transparency, dust, "noise" of the electronics, etc. A variable background is caused by a variety of factors acting throughout the reaction, such as grinding of the plastic to the thermoblock, nonspecific degradation of the labeled probes, etc. [45, 47, 48]. In the majority of cases, a variable background makes a near-linear contribution to the curves generated by the amplifier and may be subtracted without distorting the data considerably (Fig. 5).

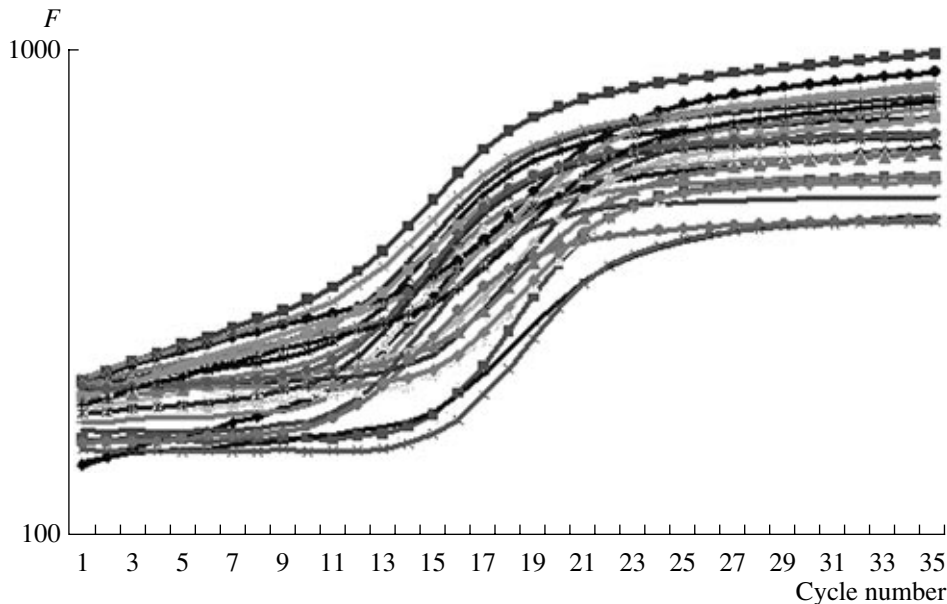The majority of software packages currently used for data analysis share the common error of an incorrect

Fig. 4. Raw DNA accumulation graphs. Each curve corresponds to one reaction tube.
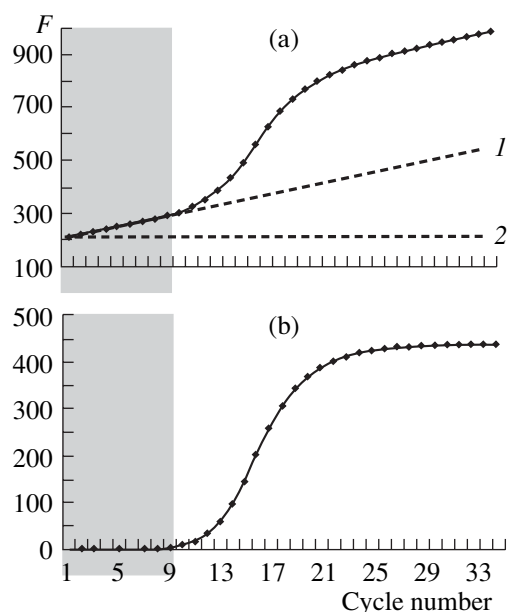
Fig. 5. Appearance of DNA accumulation graphs prior to (a) and following (b) background subtraction. The region for background fluorescence determination is shown in dark.

ground calculation (Figs. 6a and 6b), the transformation may give a graph like that shown in Fig. 6c. Figure 6d presents the same graphs with a correct background subtraction for the first curve.

A correct approach, avoiding the above problems, makes it possible to analyze each curve individually for the subsequent estimation and subtraction of background fluorescence [45].

Normalization of the factor α. The difference in the values of factor α is yet another obstacle to correct a comparison of the results (Fig. 7). As indicated above the value of α may vary both between experiments and between samples within the same experiment (one PCR run). A difference in these values may result in considerable distortion of the curves obtained [45, 49]. The main reasons for such a difference include the heterogeneity of the instrument optics; heterogeneity of optical properties of amplification tubes, dust, dirt, and the presence of fluorescent admixtures in the samples.

Even on the assumption that engineers had succeeded in designing an ideal instrument and ideal (absolutely identical) tubes, the effects of points three and four can not have been ruled out. The majority of manufacturers of detecting amplifiers are currently aware of the fact that upgrades of equipment and consumables that are not supported by sophisticated mathematical analysis of the data will not solve the problem of nonuniformity of factor α. Indeed, a good algorithm for equalization of α factors makes it possible to use in the instruments optical schemes with considerable heterogeneity.

estimation of the background component. This error is due to the fact that the zone selected for the background estimation is fixed for all curves. In the case of nonstandard curves, this approach leads to considerable distortion of the results (Fig. 6). If the software analyzing raw data incorrectly selects the zone for back-
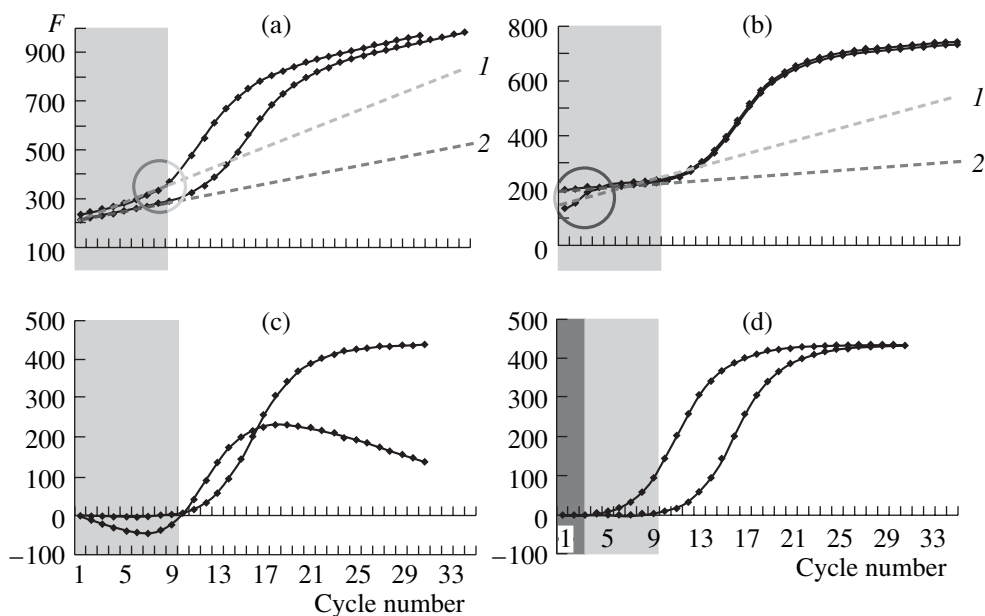

Fig. 6. Examples of the analysis of DNA accumulation graphs. Mistakes in selecting the region for background determination, i.e., covering the exponential segment (a) or the out-of-order portion at the start of the curve (b), result in considerable data distortion (c). Such problems are avoided if each curve is analyzed individually (d). Circles show regions mistakenly selected by the software. Regions for background fluorescence determination are shown in dark.
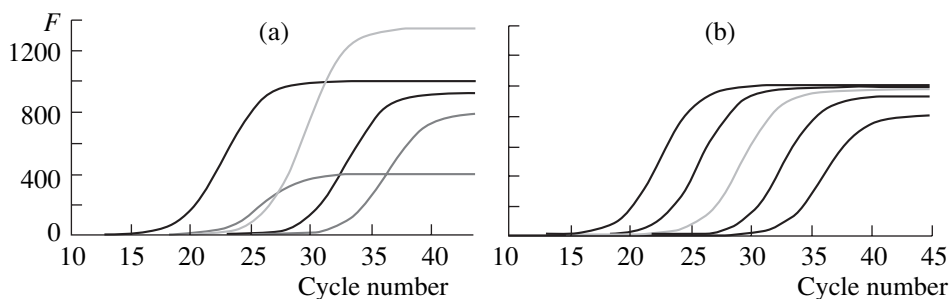
Fig. 7. Appearance of DNA accumulation graphs prior to (a) and following (b) normalization of factors α.

At present, manufacturers of the equipment use several approaches to attenuating the effects of factor α, which may be separated into two groups: (1) pretransformation of the curves for subsequent determination of C_t (using the threshold-line method) and (2) direct comparison of the curves (using characteristic points or parameters).

Methods involving pretransformation of the curves.

1. The curves are equalized using fluorescent probes present in the tubes. This approach, implemented in the instrument from Bio-Rad (iCycler iQ Multicolor Real-Time Detection System), fails to provide sufficient information for correct signal normalization, because the latter is based on the use of a single (initial) point on the graph and the possibility of considerable changes in background fluorescence is not taken into account (one value background fluorescence is obviously not sufficient for solving equation 11).

2. The curves are equalized using a normalizing dye introduced into the tubes [50]. This approach is similar to the previous one, the only difference being that α is determined using a free fluorophore (in the patent it is referred to as the dye ROX), rather than fluorescent probes. In this case, again, a single value of background fluorescence is used, and correct signal normalization is not possible.

3. The curves are equalized using the level of the plateau in the end of the reaction (amplitude normalization). In this approach, multiplication by various factors is used to reduce the levels of the plateau to the same value for all the curves. Such multiplication gives good results when the curves having different scales are characterized by identical E values and the final DNA concentrations in the tubes are the same. If the E values of the samples compared are different, the procedure aggravates the distortion [49].

Direct comparison methods of the results by the graph shape.

These include approaches based on the use of the first and second derivatives of DNA accumulation graphs [44, 46, 51]. This technique gives more reliable results, because it allows the value of factor α to be neglected. In order to compare the results directly, it is necessary to find a characteristic point on the graph, the position of which reflects the shape of the curve. Approaches developed thus far use the maximum of the first or second derivative for such a point. The advantage of using the derivatives consists in the fact that the multiplication of the curve (whatever the factors might be) does not change the position of the maxima of the derivatives. The use of the maximum of the second derivative is convenient, because, in the majority of cases, it is confined to a zone with a constant E (unless slight changes in the efficiency, inherent in PCR, are taken into account) (Fig. 8). Roche, a leader in the development of qPCR methodology, implement this approach in their instruments (Light-Cycler Real-Time PCR Cycler) as a basic analytical method of amplification results [51]. In practice, the use of the first derivative is less advantageous, because its maximum usually falls within a zone of considerable E distortion. Strictly speaking, it is not mandatory to use the maxima of the derivatives. Any characteristic point is appropriate for comparing the curves. Unlike the threshold method, in which the value characterizing the curve is termed the threshold cycle (C_t), methods of direct comparison are based on the use of the crossing point (C_p) [16, 39, 52].
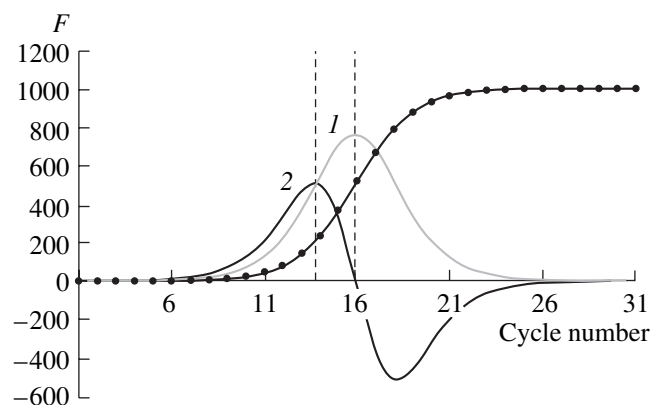

Fig. 8. DNA accumulation graph, the first (*1*) and second (*2*) derivatives of the graph. Vertical dotted lines designate the positions of maxima of the first and second derivatives.

Approaches reviewed herein do not exhaust the diversity of methods used for analyzing the results of real-time PCR. We also refrained from discussing mathematical aspects of the transformations used in detail. The audience of this work is researchers using qPCR in everyday practice, seeking to better understand specific features of both the method and the results obtained.

REFERENCES

1. Walker, N.J., *Science,* 2002, vol. 296, no. 5567, pp. 557–559.

2. Lay, M.J. and Wittwer, C.T., *Clin. Chem.*, 1997, vol. 43, no. 12, pp. 2262–2267.

3. Aslanidis, C., Nauck, M., and Schmitz, G., *BioTechniques*, 1999, vol. 27, no. 2, pp. 234–238.

4. Bustin, S.A., *J. Mol. Endocrinol*, 2000, vol. 25, no. 2, pp. 169–193.

5. Schmittgen, T.D., *Methods*, 2001, vol. 25, no. 4, pp. 383–385.

6. Giulietti, A., Overbergh, L., Valckx, D., Decallonne, B., Bouillon, R., and Mathieu, C., *Methods*, 2001, vol. 25, no. 4, pp. 386–401.

7. Feinberg, M., Fernandez, S., Cassard, S., and Bertheau, Y., *J. AOAC Int.*, 2005, vol. 88, no. 2, pp. 558–573.

8. Holland, P.M., Abramson, R.D., Watson, R., and Gelfand, D.H., *Proc. Natl. Acad. Sci. USA*, 1991, vol. 88, no. 16, pp. 7276–7280.

9. Tyagi, S. and Kramer, F.R., *Nat. Biotechnol*, 1996, vol. 14, no. 3, pp. 303–308.

10. Morrison, T.B., Weis, J.J., and Wittwer, C.T., *BioTechniques*, 1998, vol. 24, no. 6, pp. 954–958.

11. Winn-Deen, E.S., *Mol. Diagn*, 1998, vol. 3, no. 4, pp. 217–222.

12. Thelwell, N., Millington, S., Solinas, A., Booth, J., and Brown, T., *Nucleic Acid Res.*, 2000, vol. 28, no. 19, pp. 3752–3761.

13. Livak, K.J. and Schmittgen, T.D., *Methods*, 2001, vol. 25, no. 4, pp. 402–408.

14. Liu, W. and Saint, D.A., *Anal. Biochem.*, 2002, vol. 302, no. 1, pp. 52–59.

15. Bar, T., Stahlberg, A., Muszta, A., and Kubista, M., *Nucleic Acid Res.*, 2003, vol. 31, no. 17.

16. Pfaffl, M.W., *Nucleic Acid Res.*, 2001, vol. 29, no. 9.

17. Teo, I.A., Choi, J.W., Morlese, J., Taylor, G., and Shaunak, S., *J. Immunol. Methods*, 2002, vol. 270, no. 1, pp. 119–133.

18. Ball, T.B. and Plummer, F.A., HayGlass K.T, *Int. Arch. Allergy Immunol,* 2003, vol. 130, no. 1, pp. 82–86.

19. Bolufer, P., Colomer, D., Gomez, M.T., Martinez, J., Gonzalez, S.M., Gonzalez, M., Nomdedeu, J., Bellosillo, B., Barragan, E., Lo-Coco, F., Diverio, D., Hermosin, L., Garcia-Marco, J., DeJuan, M.D., Barros, F., Romero, R., and Sanz, M.A., *Clin. Chem.*, 2004, vol. 50, no. 6, pp. 1088–1092.

20. Burkardt, H.J., *Clin. Chem. Lab. Med*, 2000, vol. 38, no. 2, pp. 87–91.

21. Peters, I.R., Helps, C.R., Hall, E.J., and Day, M.J., *J. Immunol. Methods,* 2004, vol. 286, nos. 1-2, pp. 203–217.

22. Wilhelm, J., Pingoud, A., and Hahn, M., *Anal. Biochem.*, 2003, vol. 317, no. 2, pp. 218–225.

23. Muller, P.Y., Janovjak, H., Miserez, A.R., and Dobbie, Z., *BioTechniques*, 2002, vol. 32, no. 6, pp. 1372–1379.

24. Peirson, S.N., Butler, J.N., and Foster, R.G., *Nucleic Acid Res.*, 2003, vol. 31, no. 14.

25. Mullis, K., Faloona, F., Scharf, S., Saiki, R., Horn, G., and Erlich, H., *Cold Spring Harb. Symp. Quant. Biol,* 1986, vol. 51, no. 1, pp. 263–273.

26. Nogva, H.K. and Rudi, K., *BioTechniques*, 2004, vol. 37, pp. 246–253.

27. Bustin, S.A, in *A-Z of Quantitative PCR*, Tsigelny, I.S., Ed., La Jolla (USA): Int. Univ. Line, 2003, p. 7.

28. Rutledge, R.G. and Cote, C., *Nucleic Acid Res.,* 2003, vol. 31, no. 16.

29. Arezi, B., Xing, W., Sorge, J.A., and Hogrefe, H.H., *Anal. Biochem.*, 2003, vol. 321, no. 2, pp. 226–235.

30. Sikorsky, J.A., Primerano, D.A., Fenger, T.W., and Denvir, J., *Biochem. Biophys. Res. Commun.*, 2004, vol. 323, no. 3, pp. 823–830.

31. Hunt, M., *Real Time PCR. Microbiology and Immunology On-Line*, Columbia, (USA): Univ. South Carolina, 2005, pp. 1–15.

32. Liu, W. and Saint, D.A., *Biochem. Biophys. Res. Commun.*, 2002, vol. 294, no. 2, pp. 347–353.

33. Lukyanov, K.A., Matz, M.V., Bogdanova, E.A., Gurskaya, N.G., and Lukyanov, S.A., *Nucleic Acid Res.*, 1996, vol. 24, no. 11, pp. 2194–2195.

34. Liss, B., *Nucleic Acid Res.*, 2002, vol. 30, no. 17, p. e89.

35. Hartshorn, C., Anshelevich, A., and Wangh, L.J., *BMC Biotechnol*, 2005, vol. 5, no. 1, p. 2.

36. Pfaffl, M.W, in *Rapid Cycle Real-time PCR, Methods and Applications*, Meuer, S., Wittwer, C., and Nakagawara, K., Eds., Heidelberg: Springer Press, 2001, pp. 1–12.

37. Ramakers, C., Ruijter, J.M., Deprez, R.H., and Moorman, A.F., *Neurosci. Lett.*, 2003, vol. 339, no. 1, pp. 62–66.

38. Wilhelm, J. and Pingoud, A., *Chembiochem.*, 2003, vol. 4, no. 11, pp. 1120–1128.

39. Rasmussen, R., in *Rapid Cycle Real-time PCR, Methods and Applications*, Meuer, S., Wittwer, C., and Nakagawara, K., Eds., Heidelberg: Springer Press, 2001, pp. 21–34.

40. Stahlberg, A., Aman, P., Ridell, B., Mostad, P., and Kubista, M., *Clin. Chem.*, 2003, vol. 49, no. 1, pp. 51–59.

41. Peccoud, J. and Jacob, C., in *Statistical Estimations of PCR Amplification Rates. Gene Quantification*, Ferre, F., Ed., New York: Birkhauser, 1998, pp. 111–128.

42. Shiao, Y.H., *BMC Biotechnol.*, 2003, vol. 3, no. 12, p. 22.

43. Tichopad, A., Dzidic, A., and Pfaffl, M.W., *Biotechnol. Lett.*, 2002, vol. 24, no. 4, pp. 2053–2056.

44. Tichopad, A., Dilger, M., Schwarz, G., and Pfaffl, M.W., *Nucleic Aids Res*, 2003, vol. 31, no. 20, p. e122.

45. Rutledge, R.G., *Nucleic Acid Res.*, 2004, vol. 32, no. 22, p. e178.

46. Zhao, S. and Fernald, R.D., *J. Comput. Biol*, 2005, vol. 12, no. 8, pp. 1047–1064.

47. Schoder, D., Schmalwieser, A., Schauberger, G., Kuhn, M., Hoorfar, J., and Wagner, M., *Clin. Chem.*, 2003, vol. 49, no. 6, pp. 960–963.

48. Schoder, D., Schmalwieser, A., Schauberger, G., Hoorfar, J., Kuhn, M., and Wagner, M., *J. Clin. Microbiol.*, 2005, vol. 43, no. 6, pp. 2724–2728.

49. Larionov, A., Krause, A., and Miller, W., *BMC Bioinformatics*, 2005, vol. 6, no. 1, p. 62.

50. US Patent no. 20 050 227 257, 2005.

51. Cichocki, L., Hecking, C., Bareza, N., Gasser, S., Pilger, E., Klein, W., and Gasser, R., *J. Clin. Basic Cardiol,* 2004, vol. 7, nos. 1-4, pp. 26–27.

52. Pfaffl, M.W., Horgan, G.W., and Dempfle, L., *Nucleic Acid Res.*, 2002, vol. 30, no. 9, p. e36.